



## NRC Publications Archive Archives des publications du CNRC

### **Separation performance of asymmetric membranes based on PEGDa/PEI semi interpenetrating polymer network in pure and binary gas mixtures of CO<sub>2</sub>, N<sub>2</sub> and CH<sub>4</sub>**

Saimani, Sundar; Dal-Cin, Mauro M.; Kumar, Ashwani; Kingston, David M.

This publication could be one of several versions: author's original, accepted manuscript or the publisher's version. / La version de cette publication peut être l'une des suivantes : la version prépublication de l'auteur, la version acceptée du manuscrit ou la version de l'éditeur.

For the publisher's version, please access the DOI link below. / Pour consulter la version de l'éditeur, utilisez le lien DOI ci-dessous.

#### **Publisher's version / Version de l'éditeur:**

<https://doi.org/10.1016/j.memsci.2010.06.045>

*Journal of membrane science*, 362, October, pp. 353-359, 2010

#### **NRC Publications Record / Notice d'Archives des publications de CNRC:**

<https://nrc-publications.canada.ca/eng/view/object/?id=8f56342f-5224-4cf4-9e3f-2ca82cc40bbe>

<https://publications-cnrc.canada.ca/fra/voir/objet/?id=8f56342f-5224-4cf4-9e3f-2ca82cc40bbe>

Access and use of this website and the material on it are subject to the Terms and Conditions set forth at

<https://nrc-publications.canada.ca/eng/copyright>

READ THESE TERMS AND CONDITIONS CAREFULLY BEFORE USING THIS WEBSITE.

L'accès à ce site Web et l'utilisation de son contenu sont assujettis aux conditions présentées dans le site

<https://publications-cnrc.canada.ca/fra/droits>

LISEZ CES CONDITIONS ATTENTIVEMENT AVANT D'UTILISER CE SITE WEB.

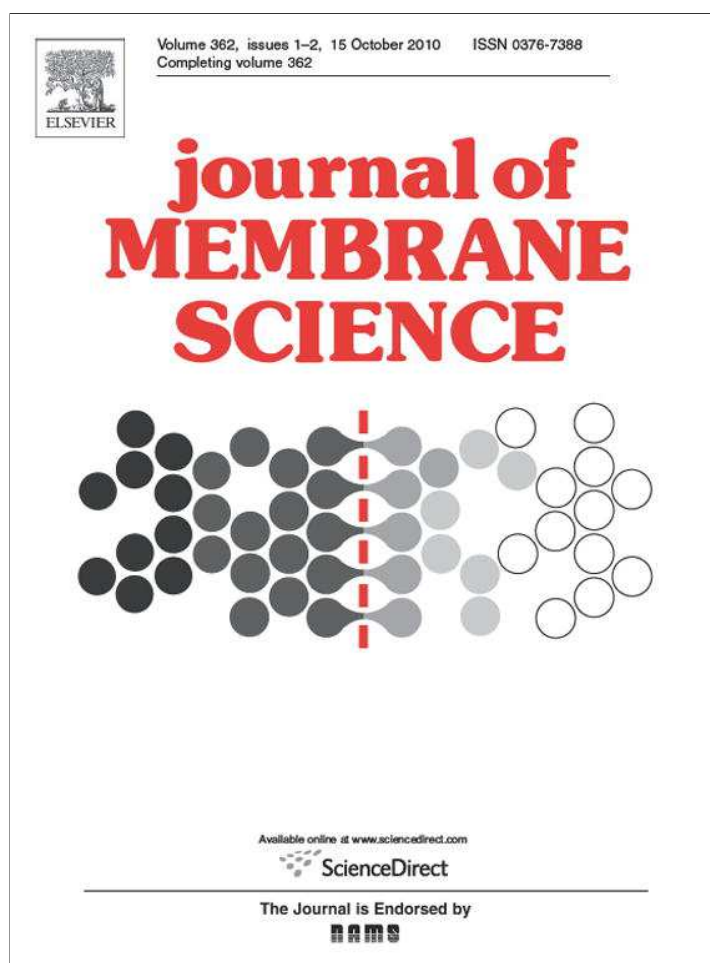
#### **Questions?** Contact the NRC Publications Archive team at

PublicationsArchive-ArchivesPublications@nrc-cnrc.gc.ca. If you wish to email the authors directly, please see the first page of the publication for their contact information.

**Vous avez des questions?** Nous pouvons vous aider. Pour communiquer directement avec un auteur, consultez la première page de la revue dans laquelle son article a été publié afin de trouver ses coordonnées. Si vous n'arrivez pas à les repérer, communiquez avec nous à PublicationsArchive-ArchivesPublications@nrc-cnrc.gc.ca.



Provided for non-commercial research and education use.  
Not for reproduction, distribution or commercial use.



This article appeared in a journal published by Elsevier. The attached copy is furnished to the author for internal non-commercial research and education use, including for instruction at the authors institution and sharing with colleagues.

Other uses, including reproduction and distribution, or selling or licensing copies, or posting to personal, institutional or third party websites are prohibited.

In most cases authors are permitted to post their version of the article (e.g. in Word or Tex form) to their personal website or institutional repository. Authors requiring further information regarding Elsevier's archiving and manuscript policies are encouraged to visit:

<http://www.elsevier.com/copyright>



Contents lists available at ScienceDirect

## Journal of Membrane Science

journal homepage: [www.elsevier.com/locate/memsci](http://www.elsevier.com/locate/memsci)

# Separation performance of asymmetric membranes based on PEGDa/PEI semi-interpenetrating polymer network in pure and binary gas mixtures of CO<sub>2</sub>, N<sub>2</sub> and CH<sub>4</sub><sup>☆</sup>

Sundar Saimani, Mauro M. Dal-Cin<sup>\*</sup>, Ashwani Kumar, David M. Kingston

National Research Council of Canada, Institute for Chemical Process and Environmental Technology, Montreal Road Campus, Ottawa, Ontario K1A 0R6, Canada

## ARTICLE INFO

## Article history:

Received 25 February 2010

Received in revised form 20 April 2010

Accepted 28 June 2010

Available online 3 August 2010

## Keywords:

Polyimides

semi-Interpenetrating polymer networks (semi-IPNs)

Poly (ethylene glycol) diacrylate

Gas permeation and plasticization

Binary gas mixtures

## ABSTRACT

Asymmetric membranes of semi-interpenetrating polymer networks (semi-IPN) were prepared with commercial poly (ether imide) (ULTEM<sup>®</sup>) and poly (ethylene glycol) diacrylate (PEGDa) in 1-methyl-2-pyrrolidinone (NMP). The selectivity and permeance of pure and mixed gases using carbon dioxide (CO<sub>2</sub>) feed concentrations of 10–40% in nitrogen (N<sub>2</sub>) or methane (CH<sub>4</sub>) were measured by the constant pressure and variable volume method at an absolute feed pressure of 1.35 MPa and 22 °C. The pure gas selectivity matched the mixed gas selectivity values at different feed concentrations, which indicated absence of plasticization. The fugacity based CO<sub>2</sub>/N<sub>2</sub> selectivity of a semi-IPN with 6% PEGDa solids content reached 50 ± 4, which is comparable to the pure gas selectivity of a dense PEGDa film ( $\alpha = 54$ ) and is significantly higher than the dense film selectivity of PEI ( $\alpha = 28$ ). The selectivity for CO<sub>2</sub>/CH<sub>4</sub> mixtures is 43 ± 10, comparable to the dense film properties of PEI ( $\alpha = 39$ ) and not the dense film selectivity of PEGDa ( $\alpha = 20$ ). The PEGDa/PEI semi-IPN membranes displayed synergistic properties, where the selectivity approached the higher value of the two materials used in making the semi-IPNs.

© 2010 Published by Elsevier B.V.

## 1. Introduction

The industry driven economy is continuously increasing the emission of carbon dioxide (CO<sub>2</sub>), which remains a major threat to global ecological stability. Apart from CO<sub>2</sub> capture and sequestration, the increasing demand for natural gas warrants economical methods for natural gas sweetening [1–4]. Industrial flue gases and raw natural gas contain significant amounts of CO<sub>2</sub>. It is mandatory to remove the CO<sub>2</sub> from other gas mixtures to either meet the upcoming strict environmental regulations or to meet pipeline specifications [5]. The separation of CO<sub>2</sub> from gas mixtures is usually achieved by absorption, adsorption, and cryogenic distillation techniques [1–4]. The economical advantages along with lower maintenance and space requirements are making membrane technology a popular choice for gas separations [1–4]. Also, hybridization of membrane technology with conventional methods to achieve superior performance is possible [6]. High selectivity and permeance are obviously desirable; however the selection of a membrane material should be such that the mixed gas selectivity is not compromised for permeance under the operating conditions of the process. Several polymer materials have been reported for

gaseous separations, however only few polymers are currently used in industry [1–4].

Gas permeation properties for any membrane material are affected by competitive sorption and plasticization [7]. These properties often vary with the structure and thickness of the membrane and the presence of other components in the gas mixtures [8]. Most of the reported literature is on permeation of single gases through thick dense films. These values, though suitable for predicting the polymer material's behavior, may vary in real time applications. There are relatively few mixed gas experiments reported on asymmetric membranes, which is the membrane configuration ultimately used in industrial applications. Since the selective layer thickness of asymmetric membranes is often less than 1 μm, their transport properties may be significantly different from dense films. Studying the transport behavior of membrane materials in the configuration to be used in an industrial application will help to elucidate the potential of the material.

Glassy polymers like polyimides, polysulfones and cellulose acetates are often preferred in industrial gaseous separations, including natural gas sweetening [1,2]. They offer higher thermal and mechanical stability, better permeance and longevity [1–4]. A polymer with a rigid backbone generally exhibits higher mobility selectivity because it will behave more like a molecular sieve [9]. Moreover, polymers with high glass transition temperatures ( $T_g$ ) can be used at higher pressure and temperature without physical deformation. These polymers are, however, susceptible to plasti-

<sup>☆</sup> NRCC No. 52224.

<sup>\*</sup> Corresponding author. Tel.: +1 613 993 0415; fax: +1 613 941 2529.

E-mail address: [mauro.dal-cin@nrc-cnrc.gc.ca](mailto:mauro.dal-cin@nrc-cnrc.gc.ca) (M.M. Dal-Cin).

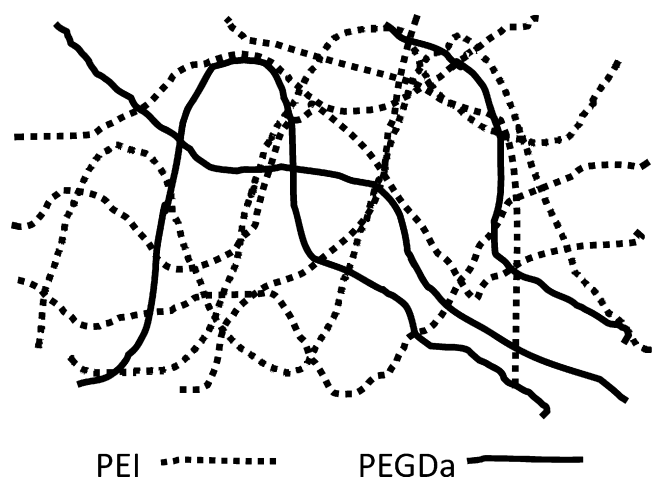


Fig. 1. Schematic representation of an IPN composed of two components A and B which are intermingled at the molecular level.

cization and thereby reduced selectivity could be observed with gas mixtures [10,11]. Commercially important glassy polymeric membranes should be improved in terms of selectivity to compete with conventional processes, particularly in view of selectivity losses with mixed gases. Poly (ethylene glycol) (PEG) based polymers exhibit good  $\text{CO}_2/\text{N}_2$  selectivity ( $\alpha \geq 50$ ), because of the higher solubility of  $\text{CO}_2$  in polar PEG [12–16]. Hence PEG is considered an attractive material for separation of  $\text{CO}_2$  from other gases. Moreover cross-linked PEGDa dense films do not show a pronounced selectivity loss due to plasticization, since the selectivity is based on solubility rather than on mobility [13].

It would be advantageous to combine these different materials, glassy polymers and PEG to get synergistic properties. These materials have been combined in different ways that include: copolymerizing amino terminated glycols [17], blending and cross-linking [18]. Copolymerization and cross-linking require tailor-made polymers, whereas blending often results in inferior properties because of phase separation. Interpenetrating polymer networks (IPNs) can be prepared from commercial materials. Due to the formation of a network structure where the polymers are interlaced at least partially at the molecular level, Fig. 1, IPNs can resist phase separation better than simple blending. Also, IPNs are reported to suppress plasticization in glassy polymers along with increasing the productivity of the material [19].

Our lab reported semi-IPN membranes having 15 times higher permeance than the parent polymers without a significant decrease in gas selectivity [20–23]. Recently we have reported the pure gas permeation studies based on semi-IPN membranes of commercially important glassy polymers and poly (ethylene glycol) diacrylate (PEGDa) [24,25]. These IPNs are formed by the cross-linking of PEGDa in a pre-polymerized component (PEI) with no covalent bonding between PEGDa and PEI; hence they fall under the category of sequential IPNs [26]. At the PEGDa concentration used in the current work, 2–8% solids, the gel content could not be measured. The PEGDa and PEI can be separated by extraction, without breaking chemical bonds and hence are classified as sequential

semi-IPNs [26]. Low et al. [27] were able to produce dense film semi-IPNs using higher concentrations, 10–50%, of cross-linked azides in 6FDA-NDA. The gel content could only be measured at 30 and 50% azide. Henceforth the IPNs produced in this work are referred to as semi-IPNs for consistency with our previous work. Based on these results, selected formulations were further studied for mixed gas separation properties. This work reports the binary gas separation performance of poly (ether imide) (PEI) and PEGDa based semi-IPN asymmetric membranes.

## 2. Theory

The pure gas selectivity,  $\alpha_{A/B}$ , of a dense film is defined by the ratio of the permeabilities ( $P$ ):

$$\alpha_{A/B} = \frac{P_A}{P_B} \quad (1)$$

where A is the gas with the higher permeability. When using an asymmetric membrane, the pure gas permeability is replaced by the permeance:

$$\alpha_{A/B}^* = \frac{P'_A}{P'_B} \quad (2)$$

and the permeance is defined as the volumetric flux per unit area per unit driving force. For mixed gases, the permeance for gas A is given by

$$P'_A = \frac{J_{\text{perm}} \times y_A}{f_{A,\text{feed}} - f_{A,\text{perm}}} \quad (3)$$

where  $J_{\text{perm}}$  is the volumetric flux in  $\text{m}^3 (\text{STP}) \text{m}^{-2} \text{s}^{-1}$ ,  $y_A$  is the mole fraction of gas A in the permeate and  $f_A$  is the absolute fugacity in the feed or permeate in Pa. Fugacity values were calculated using REFPROP, version 8.0, software supplied by the National Institute of Standards and Technology (NIST), USA.

## 3. Experimental

### 3.1. Materials

A complete description of the materials is given in a previous publication [25]. Aromatic PEI Ultem® 1000, anhydrous 1-methyl-2-pyrrolidinone (NMP), PEGDa (mol. wt. 700), benzophenone, anhydrous ethyl alcohol and hexanes are used in the study. Ultra high purity nitrogen, carbon dioxide, oxygen, methane and  $\text{CO}_2$  free/dry air were purchased from BOC Gases Canada Ltd. and were used as received without further purification.

### 3.2. Polyimide and PEGDa semi-IPN membrane preparation

The chemical structures of the various compounds and the compositions used in this study are given in Fig. 2 and Table 1 respectively. The membrane making process was previously described in detail [25], briefly, the PEI is pre-dissolved in NMP, to which the PEGDa/initiator are then added. Solutions were mixed by rolling until the onset of turbidity, then cast onto a glass plate using a doctoring blade set to 250  $\mu\text{m}$  followed by gelation into

Table 1  
Casting solution formulations for the control PEI and PEGDa/PEI semi-IPN membranes.

S. No	Membrane code	PEGDa (g)	PEI (g)	Initiator (g)	NMP (mL)	%PEGDa
1	PEI	0.00	34	0	80	0%
2	PEGDa/PEI-2%	0.68	34	0.01	80	2%
3	PEGDa/PEI-4%	1.36	34	0.01	80	4%
4	PEGDa/PEI-6%	2.04	34	0.01	80	6%
5	PEGDa/PEI-8%	2.72	34	0.01	80	8%

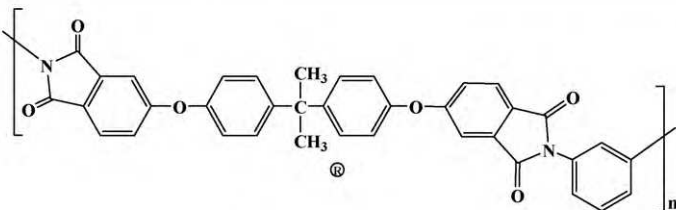
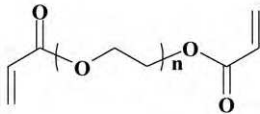
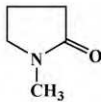
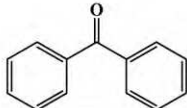
S.No	NAME	CHEMICAL STRUCTURE
1	PEI	
2	PEGDa	
3	NMP	
4	BENZO PHENONE	

Fig. 2. Chemical structures of the compounds used in this study: (1) poly (ether imide), (2) poly (ethylene glycol) diacrylate, (3) 1-methyl-2-pyrrolidinone and (4) benzophenone.

distilled water at room temperature. The water was exchanged for three consecutive days before air drying.

Membranes were coated with a 3 wt.% poly (dimethyl siloxane) (PDMS) solution (Sylgard 184) with a catalyst to base rubber ratio of 1:10 in n-pentane. Four coatings were applied holding the sample at different points to ensure complete coverage allowing the solvent to evaporate between coatings. Intermediate coatings were not cured. Finally, the PDMS coated membranes were cured in an air purging convection oven at 80 °C for one day. The membranes are identified by the weight percentage of PEGDa in PEI and PEGDa excluding the solvent.

### 3.3. Measurements

The experimental details of Attenuated Total Reflectance-Fourier Transform-Infrared (ATR-FT-IR) and scanning electron microscopy (SEM) are described in a previous publication [25]. X-ray photoelectron spectroscopy (XPS) experiments were carried out using a Kratos AXIS Ultra X-ray Photoelectron Spectrometer equipped with a hemispherical analyzer, a DLD (Delay Line Detector), charge neutralizer and a monochromatic Al K $\alpha$  X-ray source. Analyses were performed using an accelerating voltage of 14 kV and a current of 10 mA. Survey scans were performed at a pass-energy of 160 eV. Species detected using the survey scan were then analyzed at a pass-energy of 40 eV and quantified.

A cross-flow test cell having a permeation surface area of 9.6 cm<sup>2</sup> was used [28]. A feed pressure of 1.35 MPa and temperature of 22 °C was used for both single and mixed gas permeation studies. The retentate was set at a flow rate of  $6.6 \times 10^{-6}$  m<sup>3</sup>(STP) s<sup>-1</sup> for mixed gas permeation experiments and the permeate was discharged to atmosphere. The permeate flow rate was measured by a soap bubble flow meter and the CO<sub>2</sub> concentration of feed and permeate gas mixtures were determined by an infrared based analyzer (Quantek Instruments Oxygen/Carbon dioxide analyzer Model 902P). Mixed gas experiments used a CO<sub>2</sub> feed concentration of 10–20–30 and

40% in nitrogen or methane. All membranes were conditioned in each gas and each concentration of mixed gases over night before taking the measurements. The permeate recovery was  $\ll$ 1% for all cases to avoid concentration polarization and changing feed concentrations along the membrane surface.

## 4. Results and discussion

### 4.1. FT-IR spectroscopy

The FT-IR spectra of pure PEI and PEGDa/PEI semi-IPN asymmetric membranes are shown in Fig. 3. The absence of acrylic double

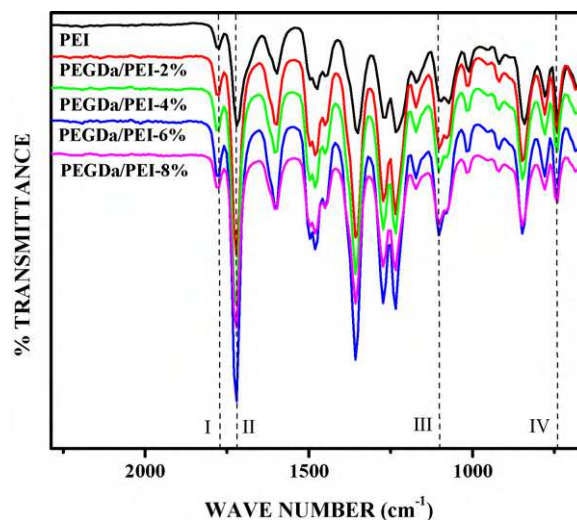
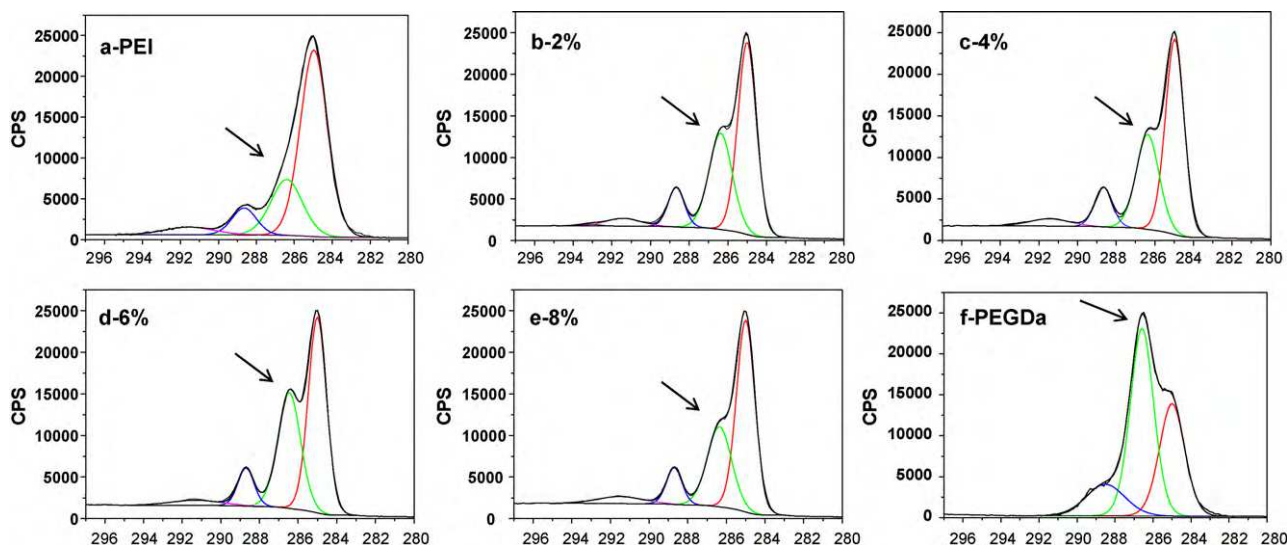


Fig. 3. ATR-FT-IR spectra of pure PEI and PEGDa/PEI semi-IPN asymmetric membranes. PEI shown at top, followed by increasing content of PEGDa up to 8% at the bottom.

**Table 2**  
ATR-FT-IR peak intensity and ratios thereof. See text for peak assignments.

Polymer	Peak I (1776 cm <sup>-1</sup> )	Peak II (1720 cm <sup>-1</sup> )	II/I	Peak III (1100 cm <sup>-1</sup> )	Peak IV (740 cm <sup>-1</sup> )	III/IV
PEI	96.9	85.0	0.88	88.7	85.8	1.03
PEGDa/PEI-2%	94.3	69.7	0.74	86.1	88.6	0.97
PEGDa/PEI-4%	94.2	67.1	0.71	88.0	91.1	0.96
PEGDa/PEI-6%	92.2	58.1	0.63	82.9	88.7	0.94
PEGDa/PEI-8%	95.6	74.2	0.78	90.1	93.5	0.96



**Fig. 4.** XPS C1s spectra of (a) control PEI, (b)–(e) semi-IPN membranes with the indicated PEGDa concentration and (f) pure PEGDa. The C–O peak at 286.4 eV is highlighted by the arrow, see text for other peak assignments.

bonds of PEGDa (1640, 1409, 1190 and 810 cm<sup>-1</sup>) [25] confirms the completion of the cross-linking reaction and thus the formation of the semi-IPN. The depth of analysis of ATR-FT-IR ranges from 200 nm at 3000 cm<sup>-1</sup> to 600 nm at 1000 cm<sup>-1</sup> [29], hence this would represent a significant fraction of the skin layer thickness which determines the permeance and selectivity.

The PEGDa content in the skin layer can be correlated with the peak ratios of absorptions which are unique to PEGDa or PEI. PEI has two absorptions for the imide carbonyl group, peaks I and II at 1776 and 1720 cm<sup>-1</sup> respectively, Fig. 3. PEGDa has one carbonyl absorption at 1720 cm<sup>-1</sup> but no absorption at 1776 cm<sup>-1</sup> [25]. The aliphatic ether >C–O–C< absorption around 1100 cm<sup>-1</sup>, peak III, is strong for PEGDa but weak for PEI. Peak IV at 740 cm<sup>-1</sup> is unique to PEI, and is due to imide ring deformation. Hence a decreasing ratio of the peaks I/II and III/IV is an indication of increasing PEGDa content in the skin layer. Examination of Table 2 shows an increasing

PEGDa content, indicated by both peak ratios, up to the PEGDa/PEI-6% formulation. A decrease of the PEGDa content is noted for the PEGDa/PEI-8% formulation. Phase separation at the highest PEGDa content may have started to happen. However, this was not indicated by DSC measurements.

#### 4.2. X-ray photoelectron spectroscopy

X-ray photoelectron spectroscopy is surface specific; sampling to a depth of 5–10 nm. XPS analysis of the reference samples (the control PEI membrane and a cross-linked dense film of PEGDa) was used to assign the characteristic absorptions of the semi-IPNs. C1s spectra of control PEI, the semi-IPN membranes and pure cross-linked PEGDa are presented in Fig. 4 and the surface elemental concentrations of C, N and O are given in Table 3. The high-resolution C1s spectra are resolved into peaks correspond-

**Table 3**  
Surface elemental concentration (C, N and O) of semi-IPN asymmetric membranes by XPS analysis.

Functional group	PEI		PEGDa/PEI-2%		PEGDa/PEI-4%		PEGDa/PEI-6%		PEGDa/PEI-8%	
	BE (eV)	ATOM %	BE (eV)	ATOM %	BE (eV)	ATOM %	BE (eV)	ATOM %	BE (eV)	ATOM %
<b>C1s</b>										
C=C, C–C	285.0	52.3	285.0	42.7	285.0	43.13	285.0	39.38	285.0	45.56
C–N, C–O	286.4	18.3	286.4	26.9	286.4	26.67	286.4	29.1	286.4	24.64
C=O	288.7	7.0	288.7	7.7	288.7	7.25	288.7	6.8	288.7	7.25
π–π*	291.4	3.9	291.4	3.2	291.4	3.52	291.4	2.87	291.4	4.04
C-ATOM %		81.5		80.5		80.6		78.2		81.5
<b>O1s</b>										
O=C	532.1	6.68	532.1	9.06	532.1	9.8	532.1	11.71	532.1	8.89
O–C	533.3	7.49	533.3	6.51	533.3	6.2	533.3	7.18	533.3	5.99
O-ATOM %		14.2		15.6		16.0		19.0		14.9
<b>N1s</b>										
C–N	400.5	4.38	400.5	3.61	400.5	3.45	400.5	2.8	400.5	3.62
N-ATOM %		4.4		3.6		3.5		2.8		3.6

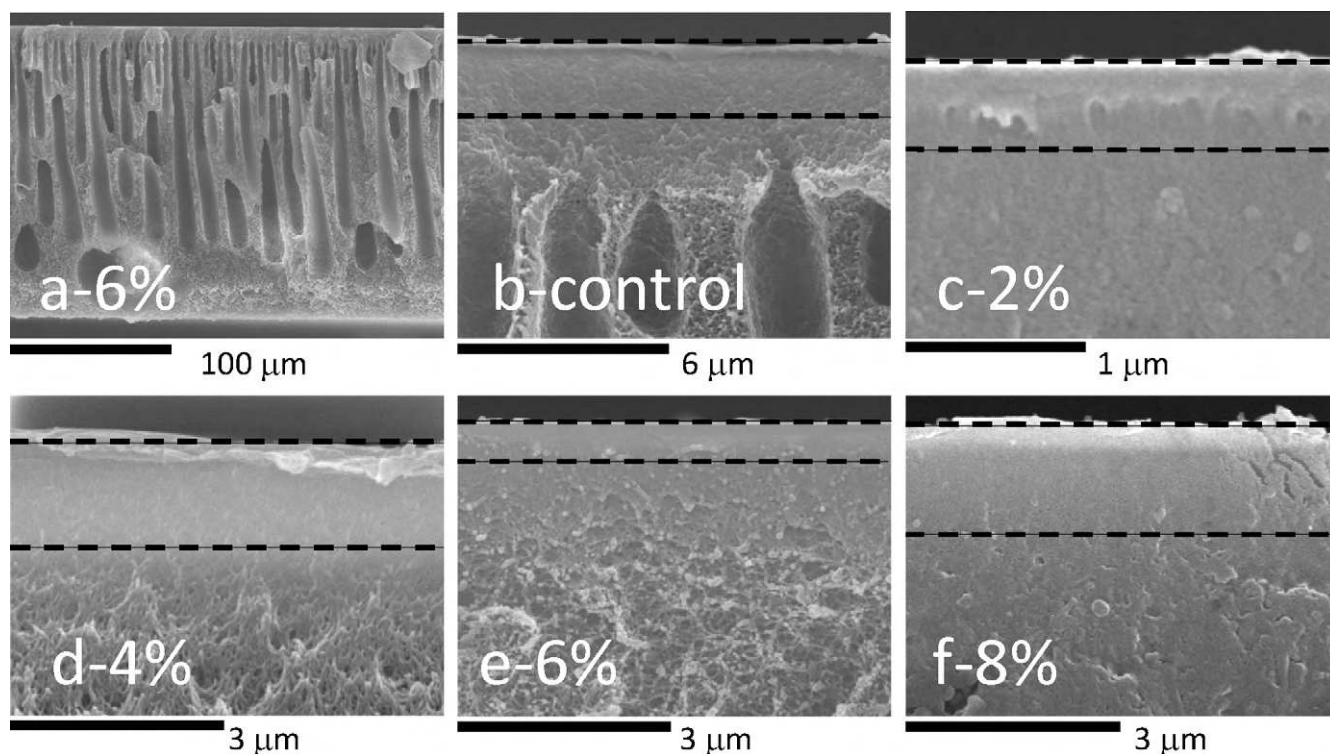


**Fig. 5.** SEMs of asymmetric membranes used in this work, no PDMS coating. Dashed lines indicate nominal skin layer thickness. (a) full cross-section view of representative membrane for PEGDa/PEI-6% and (b)–(f) control PEI and PEGDa/PEI with PEGDa concentration as indicated.

ing to those found in the literature [22,30]. In polyimides, the peak at 285.0 eV corresponds to aromatic and aliphatic carbon and the peak at 286.4 eV corresponds to carbon singly bonded to nitrogen and to oxygen. The peak at 288.7 eV is assigned to the O=C–N groups and the peak at 291.4 eV is assigned to shake up satellite of phenyl groups from  $\pi$ – $\pi^*$ . In the PEGDa dense film, the peak at 285.0 eV is assigned to C–C and the peak at 286.4 eV is assigned to C–O. The peak at 288.7 eV is assigned to C=O.

The increase in PEGDa content in the IPNs is reflected by an increase in the C–O peak at 286.4 eV, denoted by the arrow in Fig. 4(b)–(e). This peak is not resolved in pure PEI, Fig. 4(a), but is the dominant peak in the C1s spectrum of pure PEGDa, Fig. 4(f). This peak appears as a shoulder in PEGDa/PEI-2%, Fig. 4(b), while it appears as a distinct peak for PEGDa/PEI-6%, Fig. 4(d). For PEGDa/PEI-8% this peak diminishes in intensity and appears as a shoulder, Fig. 4(e).

The most obvious change is expected from core-level spectra of elemental nitrogen. PEI contains nitrogen whereas PEGDa does not, hence a decrease in the atomic percentage of nitrogen can be expected to correlate with an increasing PEGDa content. The nitrogen peak for the imide is assigned at 400.5 eV. It can be seen from Table 3 that the nitrogen concentration decreases with the addition of PEGDa, up to 6%, and then shows a slight increase for PEGDa/PEI-8%.

The theoretical atomic concentration of oxygen in PEGDa is higher than in PEI. Hence, the addition of PEGDa should increase the overall atomic concentration of oxygen in the membrane surface. The core-level O1s spectrum is curve-fitted in two peaks attributed to carbonyl oxygen at 532.1 eV and ether oxygen at 533.3 eV. It can be seen from Table 3 that the total oxygen concentration increases with increasing PEGDa content, up to PEGDa/PEI-6%.

ATR-FT-IR and XPS analysis of the membranes indicate that the PEGDa content increases with increasing PEGDa/PEI weight ratio up to 6% and then decreases for 8%. The different depths of analysis for these two techniques suggest that the PEGDa is incorporated

through a significant portion of the skin layer thickness. This could be the possible explanation of increasing selectivity for the semi-IPNs up to PEGDa/PEI-6% compared to control PEI. The PEGDa content at the surface appears to better correlate with selectivity for CO<sub>2</sub> over N<sub>2</sub> rather than the bulk content.

## 5. Membrane morphology

Based on our previous work [25], only the casting solution compositions that did not show obvious phase separations were selected for the current study. DSCs of all the compositions used in this work showed an inward shift of the  $T_g$ . Phase separation would result in two distinct glass transition temperatures corresponding to the separated components [31].

A representative scanning electron micrograph, with the full cross-section view of the PEGDa/PEI-6% semi-IPN membrane, displaying the asymmetric morphology is given in Fig. 5(a). Higher magnification images of the top layer of the control PEI, Fig. 5(b) and the semi-IPN membranes with a PEGDa content from 2 to 8% are given in (c)–(f), respectively. The transition from the dense skin layer to a porous support is highlighted with dashed lines and the approximate skin layer thickness is listed in Table 4. The membranes withstood a continuous upstream pressure of 1.35 MPa for almost 3 months without any disruption, indicating that the support layer imparted the necessary mechanical stability to the membrane.

## 6. Gas permeation studies

### 6.1. CO<sub>2</sub>/N<sub>2</sub> transport characteristics

The pure and mixed gas permeance and selectivity for CO<sub>2</sub>/N<sub>2</sub> are listed in Table 4. The average pure gas selectivity for CO<sub>2</sub>/N<sub>2</sub> increased from 23 ± 6 for the control to 48 ± 12 at 6% and then decreased to 31 ± 6 at 8%. This maximum in the pure gas selec-

**Table 4**  
Skin layer thickness, initial pure gas permeance, and estimated CO<sub>2</sub> permeability. Pure gas selectivity,  $\alpha_{\text{CO}_2/\text{N}_2}$ , and mixed gas selectivity,  $\alpha'_{\text{CO}_2/\text{N}_2}$ , of control PEI and semi-IPN membranes.

Membrane	$\delta$ (m)	Initial pure gas permeance (GPU) <sup>a</sup>	Permeability (Barrer) <sup>b</sup>	$\alpha_{\text{CO}_2/\text{N}_2}$ <sup>c</sup>	$\alpha'_{\text{CO}_2/\text{N}_2}$ <sup>d</sup>
PEI	2.1	0.65	1.4	23 ± 6	31 ± 6
PEGDa/PEI-2%	0.5	2.35	1.2	28 ± 5	35 ± 1
PEGDa/PEI-4%	1.4	1.09	1.5	24 ± 2	33 ± 2
PEGDa/PEI-6%	0.5	2.45	1.2	48 ± 12	50 ± 4
PEGDa/PEI-8%	1.4	0.74	1.0	31 ± 6	45 ± 3

<sup>a</sup> Gas permeation unit, 1 GPU =  $7.50 \times 10^{-12} \text{ m}^3(\text{STP})\text{m}^{-2} \text{ s}^{-1} \text{ Pa}^{-1}$ .

<sup>b</sup> 1 Barrer =  $7.5 \times 10^{-18} \text{ m}^3(\text{STP})\text{m}^{-1} \text{ m}^{-2} \text{ s}^{-1} \text{ Pa}^{-1}$ .

<sup>c</sup> Pure gas selectivity, average and standard deviations of three measurements, over a 3-month period.

<sup>d</sup> Mixed gas selectivity, average and standard deviation of values at 4 CO<sub>2</sub> feed concentrations, except 6% PEGDa/PEI which is the average of seven values.

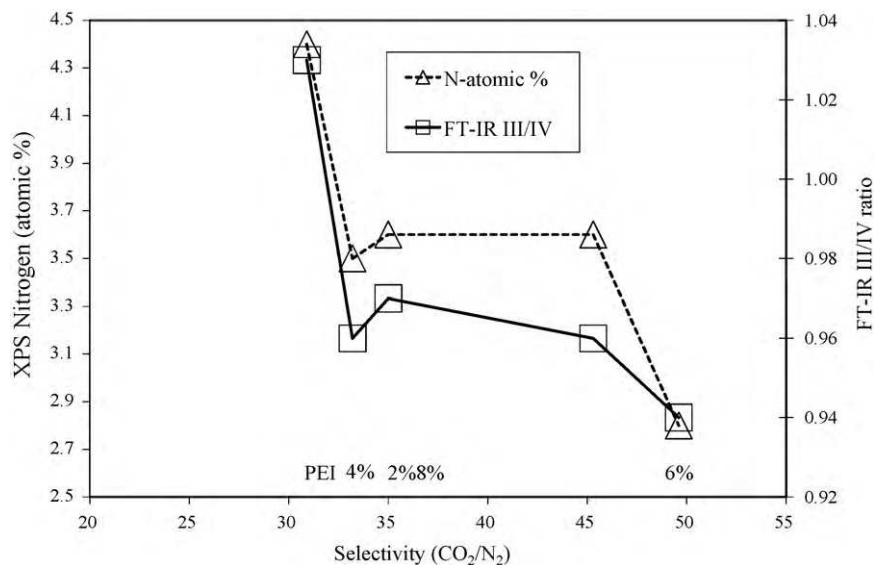


**Fig. 6.** XPS atomic nitrogen content and ratio of the III/IV FT-IR peaks as a function of the mixed gas selectivity for CO<sub>2</sub>/N<sub>2</sub> for the control PEI and PEGDa/PEI membranes as indicated above the abscissa. Decreasing nitrogen content or III/IV peak ratio indicate increasing PEGDa content in the skin layer.

tivity at PEGDa content of 6% is analogous to our previous report [25]. The average pure gas selectivity for the control PEI membrane (23 ± 6) is lower than the theoretical value (28 [4]) but is within our experimental error. The average pure gas selectivity of the PEGDa/PEI-6% membrane is 48 ± 12, which is comparable to the dense film selectivity of PEGDa.

The CO<sub>2</sub>/N<sub>2</sub> mixed gas selectivity increased from 31 ± 6 for the control membrane to a maximum value of 50 ± 4 with the PEGDa/PEI-6% membrane. There is a slight, but not significant decrease, to 45 ± 3 with the PEGDa/PEI-8% membrane. The  $\alpha'_{\text{CO}_2/\text{N}_2}$  is consistent with the PEGDa content in the skin layer rather than the bulk composition, as indicated by the decreasing XPS nitrogen content and decreasing ATR-FT-IR peak ratio (III/IV) in Fig. 6. Note that decreasing values of the XPS and ATR-FT-IR parameters indicate an increasing PEGDa content in skin layer and hence the better CO<sub>2</sub>/N<sub>2</sub> selectivity. In summary, the control, PEGDa/PEI-2% and PEGDa/PEI-4% membranes exhibit a CO<sub>2</sub>/N<sub>2</sub> selectivity that is close to or slightly better than the PEI dense film selectivity for this gas pair. A dramatic change to the CO<sub>2</sub>/N<sub>2</sub> selectivity of PEGDa dense films is achieved with the PEGDa/PEI-6% and PEGDa/PEI-8% membranes.

Plasticization with polyimides has been reported at pressures between 0.5 and 1.0 MPa, with dense films of 6FDA/mPD copolymers [18], Matrimid [11] and asymmetric hollow fibers of P84 [32]. The PEI/PEGDa semi-IPNs did not exhibit any plasticization at the pressure used in this work (1.35 MPa total pressure and 0.54 MPa CO<sub>2</sub> partial pressure). This behavior was comparable to that reported for cross-linked dense films of PEGDa [15].

Normalizing the CO<sub>2</sub> permeance by the estimated skin layer thickness yields a relatively constant permeability, ranging from 1.0 to 1.5 Barrer. Hence the permeance of the PEI-PEGDa membranes appears to be determined by the skin layer thickness and PEI properties, while the selectivity is dominated by the PEGDa content in the skin layer.

## 6.2. CO<sub>2</sub>/CH<sub>4</sub> transport characteristics

The pure gas permeance and fugacity based selectivity for CO<sub>2</sub>/CH<sub>4</sub> are summarized in Table 5. The mixed gas selectivity of the control PEI membrane is 36 ± 4, matching the literature dense

**Table 5**  
Initial pure gas permeance, pure gas selectivity,  $\alpha_{\text{CO}_2/\text{CH}_4}$ , and mixed gas selectivity,  $\alpha'_{\text{CO}_2/\text{CH}_4}$ , of control PEI and semi-IPN membranes.

Membrane	Initial pure gas permeance (GPU) <sup>a</sup>	$\alpha_{\text{CO}_2/\text{CH}_4}$ <sup>b</sup>	$\alpha'_{\text{CO}_2/\text{CH}_4}$ <sup>c</sup>
PEI	0.65	33 ± 7	36 ± 4
PEGDa/PEI-2%	2.35	30 ± 3	34 ± 6
PEGDa/PEI-4%	1.09	25 ± 3	25 ± 2
PEGDa/PEI-6%	2.45	43 ± 3	43 ± 10
PEGDa/PEI-8%	0.74	50 ± 8	54 ± 9

<sup>a</sup> Gas permeation unit, 1 GPU =  $7.50 \times 10^{-12} \text{ m}^3(\text{STP})\text{m}^{-2} \text{ s}^{-1} \text{ Pa}^{-1}$ .

<sup>b</sup> Pure gas selectivity, average and standard deviation of three measurements and standard deviation, over a 3-month period.

<sup>c</sup> Mixed gas selectivity, average of values at 4 CO<sub>2</sub> feed concentrations and standard deviation.



film pure gas selectivity of 39. The  $\alpha'_{\text{CO}_2/\text{CH}_4}$  for the PEGDa/PEI-2% is similar, while that of the PEGDa/PEI-4% is somewhat low at  $25 \pm 2$ . The mixed gas selectivity with 6 and 8% PEGDa is  $43 \pm 10$  and  $54 \pm 9$  respectively. In summary, all the formulations, with the exception of the PEGDa/PEI-4% membrane, match or slightly surpass the PEI dense film selectivity and significantly surpassing the dense film selectivity for PEGDa (20). There was no shortfall of the mixed gas selectivity in comparison to the pure gas values within experimental error, which indicated no plasticization.

### 6.3. Comparison of $\text{CO}_2/\text{N}_2$ vs $\text{CO}_2/\text{CH}_4$ selectivity

The highest  $\text{CO}_2/\text{N}_2$  mixed gas selectivity of the semi-IPNs was  $50 \pm 4$  with a PEGDa content of 6%, approaching the selectivity of pure PEGDa cross-linked dense films. This was significantly higher than the control PEI membrane with a selectivity of  $30 \pm 6$ , matching the dense film pure gas selectivity of 28. The mixed gas selectivity with  $\text{CO}_2/\text{CH}_4$  for the pure PEI control membrane is  $36 \pm 4$ , matching the dense film pure gas selectivity of 39. The membranes with 6% and 8% PEGDa content also matched or slightly surpassed the selectivity of pure PEI and clearly exceeded the PEGDa selectivity of 20 for this gas pair.

## 7. Conclusions

Asymmetric membranes with a typical skin layer supported over finger-like voids were successfully formed from semi-IPNs of commercial PEI (Ultem® 1000) and PEGDa. The formation of semi-IPNs was confirmed by the absence of acrylic absorptions in ATR-FT-IR spectra. Increase in PEGDa content in the selective layer with the addition of PEGDa was shown by ATR-FT-IR and XPS analyses. A maximum  $\text{CO}_2/\text{N}_2$  selectivity of  $50 \pm 4$  and  $\text{CO}_2$  permeance of 2.5 GPU was achieved with a PEGDa content of 6%; essentially achieving the selectivity of pure PEGDa. The  $\text{CO}_2/\text{CH}_4$  selectivity for this membrane is  $43 \pm 10$ , comparable to that of PEI, not that of PEGDa which is significantly lower at 20. The PEI/PEGDa semi-IPNs have a selectivity that is comparable to the most selective material for the  $\text{CO}_2/\text{N}_2$  (PEGDa) and  $\text{CO}_2/\text{CH}_4$  (PEI) gas pairs. Plasticization or competitive sorption was not observed for the materials in this study up to a pressure of 1.35 MPa.

## Acknowledgements

The authors are thankful to Ms. Linda Layton and Andrzej Nicalek of ICPET-NRCC for helping with experiments. Financial support from Natural Resources Canada's ecoETI and National Bio-products programs is gratefully acknowledged.

## Appendix A. Supplementary data

Supplementary data associated with this article can be found, in the online version, at doi:10.1016/j.memsci.2010.06.045.

## References

- [1] R.W. Baker, Future directions of membrane gas separation technology, *Ind. Eng. Chem. Res.* 41 (2002) 1393–1411.
- [2] S. Sridhar, B. Smitha, T.M. Aminabhavi, Separation of carbon dioxide from natural gas mixtures through polymeric membranes—a review, *Sep. Purif. Rev.* 36 (2007) 113–174.
- [3] C.E. Powell, G.G. Qiao, Polymeric  $\text{CO}_2/\text{N}_2$  gas separation membranes for the capture of carbon dioxide from power plant flue gases, *J. Membr. Sci.* 279 (2006) 1–49.
- [4] W.J. Koros, G.K. Fleming, S.M. Jordan, T.H. Kim, H.H. Hoehn, Polymeric membrane materials for solution-diffusion based permeation separations, *Prog. Polym. Sci.* 13 (1988) 339–401.
- [5] J. Hao, P.A. Rice, S.A. Stern, Upgrading low-quality natural gas with  $\text{H}_2\text{S}$ - and  $\text{CO}_2$ -selective polymer membranes: Part I. Process design and economics of membrane stages without recycle streams, *J. Membr. Sci.* 209 (2002) 177–206.
- [6] B.D. Bhide, A. Voskericyan, S.A. Stern, Hybrid processes for the removal of acid gases from natural gas, *J. Membr. Sci.* 140 (1998) 27–49.
- [7] T. Visser, N. Masetto, M. Wessling, Materials dependence of mixed gas plasticization behavior in asymmetric membranes, *J. Membr. Sci.* 306 (2007) 16–28.
- [8] R.T. Chern, W.J. Koros, E.S. Sanders, R. Yui, “Second component” effects in sorption and permeation of gases in glassy polymers, *J. Membr. Sci.* 15 (1983) 157–169.
- [9] D.R.B. Walker, W.J. Koros, Transport characterization of a polypyrrolone for gas separations, *J. Membr. Sci.* 55 (1991) 99–117.
- [10] M. Wessling, S. Schoeman, Th.V. Boomgaard, C.A. Smolders, Plasticization of gas separation membranes, *Gas Sep. Purif.* 5 (1991) 222–228.
- [11] A. Bos, I.G.M. Punt, M. Wessling, H. Strathmann,  $\text{CO}_2$ -induced plasticization phenomena in glassy polymers, *J. Membr. Sci.* 155 (1999) 67–78.
- [12] H. Lin, B.D. Freeman, Gas and vapor solubility in cross-linked poly(ethylene glycol diacrylate), *Macromolecules* 38 (2005) 8394–8407.
- [13] H. Lin, E.V. Wagner, B.D. Freeman, L.G. Toy, R.P. Gupta, Plasticization-enhanced hydrogen purification using polymeric membranes, *Science* 311 (2006) 639–642.
- [14] H. Lin, B.D. Freeman, Materials selection guidelines for membranes that remove  $\text{CO}_2$  from gas mixtures, *J. Mol. Struct.* 739 (2001) 57–74.
- [15] H. Lin, E.V. Wagner, R. Raharjo, B.D. Freeman, I. Roman, High-performance polymer membranes for natural-gas sweetening, *Adv. Mater.* 18 (2006) 39–44.
- [16] N.P. Patel, A.C. Miller, R.J. Spontak, Highly  $\text{CO}_2$ -permeable and -selective membranes derived from cross-linked poly(ethylene glycol) and its nano composite, *Adv. Mater.* 15 (2003) 729–733.
- [17] K.I. Okamoto, N. Umeo, S. Okamoto, K. Tanaka, H. Kita, Selective permeation of carbon dioxide over nitrogen through polyethyleneoxide-containing polyimide membranes, *Chem. Lett.* 22 (1993) 225–228.
- [18] C. Staudt-Bickel, W.J. Koros, Improvement of  $\text{CO}_2/\text{CH}_4$  separation characteristics of polyimides by chemical cross-linking, *J. Membr. Sci.* 155 (1999) 145–154.
- [19] A. Bos, I.G.M. Punt, M. Wessling, H. Strathmann, Suppression of  $\text{CO}_2$ -plasticization by semi-interpenetrating polymer network formation, *J. Polym. Sci. B: Polym. Phys.* 36 (1998) 1547–1556.
- [20] J. Kurdi, A. Kumar, Synthesis and characterization of modified bis-maleimide/polysulfone semi-interpenetrating polymer networks, *J. Appl. Polym. Sci.* 102 (2006) 369–379.
- [21] J. Kurdi, A. Kumar, Formation and thermal stability of BMI-based interpenetrating polymers for gas separation membranes, *J. Membr. Sci.* 280 (2006) 234–244.
- [22] J. Kurdi, A. Kumar, Structuring and characterization of a novel highly microporous PEI/BMI semi-interpenetrating polymer network, *Polymer* 46 (2005) 6910–6922.
- [23] J. Kurdi, A. Kumar, Performance of PEI/BMI semi-IPN membranes for separations of various binary gaseous mixtures, *Sep. Purif. Technol.* 53 (2006) 301–311.
- [24] S. Saimani, A. Kumar, Polyethylene glycol diacrylate and thermoplastic polymers based semi-IPNs for asymmetric membranes, *Compos. Interf.* 15 (2008) 781–797.
- [25] S. Saimani, A. Kumar, Semi-IPN asymmetric membranes based on polyimide (ULTEM®) and polyethylene glycol diacrylate for gaseous separation, *J. Appl. Polym. Sci.* 110 (2008) 3606–3615.
- [26] W.J. Work, K. Horie, M. Hess, R.F.T. Stepto, Definitions of terms related to polymer blends, composites, and multiphase polymeric materials, *Pure Appl. Chem.* 76 (2004) 1985–2007.
- [27] B.T. Low, T.S. Chung, H. Chen, Y. Jean, K.P. Pramoda, Tuning the free volume cavities of polyimide membranes via the construction of pseudo-interpenetrating networks for enhanced gas separation performance, *Macromolecules* 42 (2009) 7042–7054.
- [28] N. Kawachale, A. Kumar, D.M. Kirpalani, A flow distribution study of laboratory scale membrane gas separation cells, *J. Membr. Sci.* 332 (2009) 81–88.
- [29] D.J. Carlsson, M.M. Dal-Cin, P. Black, C.N. Lick, A surface spectroscopic study of membranes fouled by pulp mill effluent, *J. Membr. Sci.* 142 (1998) 1–11.
- [30] G. Beamson, D. Briggs, High Resolution XPS of Organic Polymers—The Scienta ESCA300 Database, John-Wiley & Sons, New York, USA, 1992.
- [31] J. Yang, M.A. Winnik, Polyurethane-polyacrylate interpenetrating networks. 2. Morphology studies by direct non-radiative energy transfer experiments, *Macromolecules* 29 (1996) 7055–7063.
- [32] J.N. Barsema, G.C. Kapantaidakis, N.F.A. van der Vegt, G.H. Koops, M. Wessling, Preparation and characterization of highly selective dense and hollow fiber asymmetric membranes based on BTDA-TDI/MDI co-polyimide, *J. Membr. Sci.* 216 (2003) 195–205.